Cement & Concrete Composites 31 (2009) 263–267

Contents lists available at ScienceDirect

Cement & Concrete Composites

journal homepage: www.elsevier.com/locate/cemconcomp

Measurement of linear thermal expansion coefficient of alkali-activated aluminosilicate composites up to 1000 °C

Lucie Zuda, Robert Černý *

Department of Materials Engineering and Chemistry, Faculty of Civil Engineering, Czech Technical University in Prague, Thákurova 7, 166 29 Prague 6, Czech Republic

ARTICLE INFO

Article history:
Received 18 March 2008
Received in revised form 2 February 2009
Accepted 3 February 2009
Available online 12 February 2009

Keywords:
Alkali-activated aluminosilicate composites
Electrical porcelain
Quartz sand
Linear thermal expansion coefficient

ABSTRACT

The effect of high temperatures up to 1000 °C on the length changes of two alkali-activated aluminosilicate composites, one of them with quartz sand aggregates, the second with electrical porcelain, is analyzed in the paper. The thermal strain vs. temperature functions of both materials are found to increase monotonically in the whole temperature range studied so that the thermal expansion mismatch (the gel undergoes thermal shrinkage, the aggregates expand with increasing temperature) results in positive values of the apparent linear thermal expansion coefficient. The composite material with electrical porcelain aggregates exhibits a more desired thermomechanical behavior which is a consequence of the better high-temperature thermal stability of electrical porcelain as compared to quartz. In a comparison with Portland-cement based composites, the linear thermal expansion coefficient of both studied aluminosilicates is substantially lower in the whole temperature range of 20–1000 °C.

1. Introduction

Alkali-activated aluminosilicates have been intensively studied over the past two decades as a promising alternative to Portland-cement based composites. The unique combination of high strength, enhanced fire resistance and good chemical resistance, which are characteristic for this type of materials (for detailed analysis see, e.g., [1–3]), has attracted many investigators active in materials science, chemical engineering and civil engineering.

Mechanical properties have been the most frequently investigated parameters of alkali-activated aluminosilicates, similarly as in the case of Portland-cement composites. In room-temperature conditions they were analyzed for instance in [4–10], and after high-temperature exposure in [11–14]. Other parameters have been studied only rarely: hydric properties were measured in [13,15], chloride diffusion in [15–17], and thermal properties in [12,18]. Volumetric changes of alkali-activated aluminosilicates were studied mostly in the hydration stage [8,9,19] as their drying and autogenous shrinkage have always been considered a serious threat. Length changes at elevated temperatures were studied for several types of geopolymers [20–22] and for alkali activated slag pastes [23]. In all cases remarkable thermal shrinkage (up to 25%) was observed.

Alkali-activated aluminosilicates can find use in such applications in building industry where elevated temperatures may be expected, such as walls and floors adjacent to various heat machines, pipes or chemical process vessels, envelopes or linings of special vessels such as coal gasification vessels, nuclear safety related structures in nuclear power plants, tunnel or shaft walls and fire-protecting linings. In all these cases volumetric changes in the high-temperature range can play a significant role. Sudden strain changes, negative strains or thermomechanical incompatibility of different parts of a structure can lead to serious damage.

In this paper, the linear thermal expansion coefficient of two alkali-activated aluminosilicate composites produced from ground granulated blast furnace slag in the temperature range up to 1000 °C is measured. Two different types of aggregates, quartz sand and electrical porcelain, are used, and their effect on thermomechanical behavior of the composites is analyzed.

2. Thermal expansion at high temperatures

In the determination of the linear thermal expansion coefficient α over a narrow temperature interval (T_0,T), which is common in normal temperature measurements, one can usually assume $\alpha = \alpha_0 = \text{const}$. Then, a single experiment is sufficient consisting of heating a specimen from the initial temperature T_0 to the final temperature T and measuring the thermal strain ε.

In wider temperature ranges, this assumption is no longer valid. The linear thermal expansion coefficient varies with temperature, $\alpha = \alpha(T)$, and for the thermal strain we have

$$\varepsilon(T) = \int_{T_0}^{T} \alpha(T)dT \tag{1}$$

* Corresponding author. Tel.: +420 224354429; fax: +420 224354446.
E-mail address: cernyr@fsv.cvut.cz (R. Černý).

0958-9465/$ - see front matter © 2009 Elsevier Ltd. All rights reserved.
doi:10.1016/j.cemconcomp.2009.02.002

In a practical experiment we then choose a reference temperature T_0, heat a specimen step by step to the temperatures T_i, $i = 1,\ldots,n$, covering the desired temperature range, and determine the corresponding values of ε_i, $i = 1,\ldots,n$,. The point-wise defined function $\varepsilon_i = f(T_i)$ is then approximated by means of regression analysis and its continuous representation $\varepsilon(T)$ is obtained. Finally, the linear thermal expansion coefficient $\alpha(T)$ is calculated as the first derivative of $\varepsilon(T)$ with respect to temperature.

3. Experimental method

Thermal expansion of solid materials in high-temperature range is measured by commercially produced dilatometers mostly. Various treatments are employed, for instance the methods based on variations of electric resistance, capacitance, inductance, or the interference methods. However, the applicability of many common methods which work with small specimen dimensions may be rather limited for building materials which are mostly nonhomogeneous. Therefore, the comparative method proposed by Toman et al. [24] which was used for various building materials in the past was employed for the measurements in this paper. As some modifications of the experimental setup were done to bring the original method up to date we will give a brief description of the method in what follows.

The measuring device for determining the linear thermal expansion of porous materials in the high-temperature range is based on the application of a comparative technique (see Fig. 1). A bar sample of the studied material is put into a cylindrical, vertically oriented electric furnace. As it is technically difficult to perform length measurements directly in the furnace, a thin ceramic rod, which passes through the furnace cover, is fixed on the topside of the measured sample. The length changes can be determined outside the furnace in this way, for instance by a digital dial indicator, but on the other hand, the temperature field in the ceramic rod is very badly defined, and it is not possible to determine directly, which part of the total change of length is due to the measured sample and due to the ceramic rod.

Therefore, the measurement is performed at the same time on the sample of a standard material (such as special steels where $\alpha(T)$ is known) which is put into the furnace together with the studied material and is provided with an identical ceramic rod passing through the over. The change of length of the ceramic rod can be determined in this way, and consequently also the length change of the measured sample.

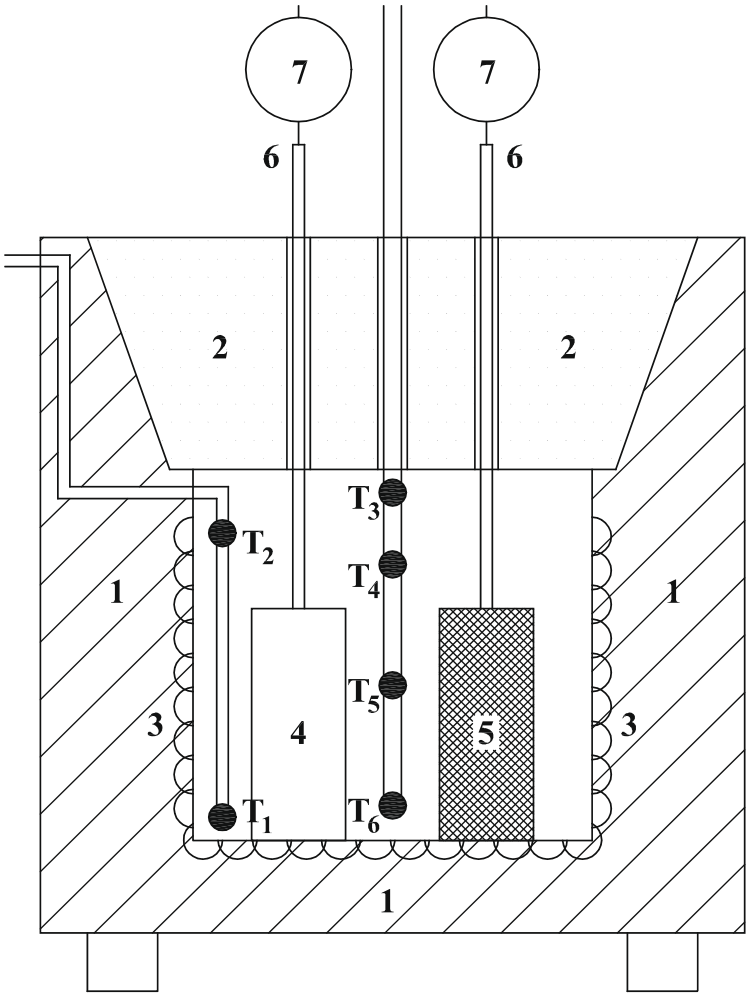

1 - furnace shell (thermal insulation), 2 - furnace cover, 3 - heating coil, 4 – standard, 5 - measured sample, 6 - ceramic rods, 7 – digital dial indicator, $T_{1\text{-}6}$ – thermocouples

Fig. 1. Scheme of the measuring device for determination of high temperature linear thermal expansion coefficient.

Table 1
Chemical composition of applied slag.

SiO_2 (%)	Fe_2O_3 (%)	Al_2O_3 (%)	CaO (%)	MgO (%)	MnO (%)	Cl^- (%)	Na_2O (%)	K_2O (%)	SO_3 (%)
38.6	0.52	7.22	38.77	12.90	0.50	0.06	0.21	0.38	0.36

It should be noted that temperature field is not constant in the whole volume of the furnace due to the differences of heat loss in the heated walls and in the cover. Therefore, temperature field in the furnace is measured by thermocouples, and an average value of temperature is considered in α calculations.

A practical measurement of the linear thermal expansion coefficient of a porous material with the device proposed in the previous section can be described as follows. The measured sample and the standard are put into the furnace, provided with contact ceramic rods, and the initial reading on the dial indicators is taken. Then, the electric heating regulation system is adjusted for the desired temperature T_i in the furnace, and the length changes are monitored. The data acquisition from the digital dial indicators is done on PC using specially developed software. After the steady state is achieved, i.e., no temperature changes in the furnace and no length changes of both measured sample and the standard are observed, the final readings of length changes are taken. The length change of the measured sample is calculated from the following formula:

$$\Delta l(T_i) = \Delta l_m(T_i) - \Delta l_s(T_i) + l_{0,s}\int_{T_0}^{Ti}\alpha_s(T)dT, \quad (2)$$

where Δl_m, Δl_s are the final readings of total length changes of the studied material and of the standard including the length changes of the ceramic rods, respectively, $l_{0,s}$ is the initial length of the standard, and α_s is the known linear thermal expansion coefficient of the standard. The corresponding value of thermal strain can be expressed in the form:

$$\varepsilon(T_i) = \frac{\Delta l(T_i)}{l_{0,m}}, \quad (3)$$

where $l_{0,m}$ is the initial length of the measured sample.

The measurements are then repeated with other chosen values of furnace temperature T_i, and the $\alpha(T)$ function of the measured material is determined using the procedure described in the previous section.

Table 2
Slag granulometry.

Sieve residue mm (%)		Specific surface (cm^2/g)
0.045	0.09	
12.4	1.9	3920

Table 3
Sand granulometry.

Sieve mesh (mm)	2	1.6	1.0	0.5	0.16	0.08
Total sieve residue (%)	0	7 ± 5	33 ± 5	67 ± 5	87 ± 5	99 ± 1

4. Materials and samples

Two composite materials on the basis of alkali activated slag were investigated. They differed in the type of aggregates. The first aggregate type was quartz sand (this material will be denoted as NS in what follows), the second electrical porcelain (EP). Fine-ground granulated blast furnace slag of Czech origin (Kotouč Štramberk, Ltd.) was used for sample preparation. Its chemical composition is shown in Table 1, its granulometry in Table 2. As alkali activator, water glass solution ($Na_2O \cdot xSiO_2 \cdot yH_2O$) was used. It was prepared using Portil-A dried sodium silicate (Na_2SiO_3) preparative (Cognis Iberia, s.l. Spain). The quartz sand aggregates were normalized according to ČSN EN 196-1 with the granulometry given in Table 3. Electrical porcelain was provided by P-D Refractories CZ, Velké Opatovice. Its porosity was 0.3%, water absorption at saturation 0.1%, bulk density 2350 kg/m^3. Chemical composition of the electrical porcelain is given in Table 4, its granulometry in Table 5.

The composition of mixtures for sample preparation is presented in Tables 6a, and b. The technology of sample preparation was as follows: First, the silicate preparative was mixed with water. The solution was then mixed in the homogenized slag–aggregate mixture. The final mixture was put into molds and vibrated. The specimens were demolded after 24 h and then stored for additional 27 days in a water bath at laboratory temperature. The dimension of the specimens was $40 \times 40 \times 100$ mm. Three specimens for each mixture were used for the measurement of linear thermal expansion coefficient.

5. Experimental results and discussion

Fig. 2 shows the measured thermal strain of both studied materials as function of temperature up to 1000 °C. The $\varepsilon(T)$ functions of

Table 4
Chemical composition of electrical porcelain.

SiO_2 (%)	Fe_2O_3 (%)	Al_2O_3 (%)	CaO (%)	MgO (%)	Na_2O (%)	K_2O (%)	TiO_2 (%)
48.6	0.8	45.4	0.3	0.2	1.0	2.9	0.7

Table 5
Electrical porcelain granulometry.

Sieve mesh (mm)	4.00	2.50	1.00	0.50	0.25	0.125	0.090	0.063	0.045
Total sieve residue (%)									
0–1 mm fraction	–	–	0.69	45.24	70.76	89.98	93.4	98.99	99.99
1–3 mm fraction	–	4.12	78.33	99.57	99.94	99.94	99.95	98.98	100.00
3–6 mm fraction	69.31	95.52	99.97	99.98	99.99	100.00	–	–	–

Table 6a
Composition of the mixture with quartz sand aggregates for sample preparation.

Sand (g)			Slag (g)	Alkali-activation silicate admixture (g)	Water (ml)
PG1	PG2	PG3			
450	450	450	450	90	190

Table 6b
Composition of the mixture with electrical porcelain aggregates for sample preparation.

Electrical porcelain (g)			Slag (g)	Alkali-activation silicate admixture (g)	Water (ml)
0–1 mm fraction	1–3 mm fraction	3–6 mm fraction			
450	450	450	450	90	190

both materials were increasing in the whole temperature range so that no thermal shrinkage was observed up to 1000 °C, contrary to the results obtained for geopolymers [20–22] and alkali activated slag pastes [23]. This difference is apparently a consequence of the presence of aggregates in the alkali-activated aluminosilicate composites studied in this paper which caused thermal expansion mismatch in the material (the gel undergoes thermal shrinkage, the aggregates expand with increasing temperature); the materials analyzed in [20–23] were pastes. This statement can be supported by the investigations in [25] where for Portland cement mortar thermal expansion was observed in the whole studied temperature range of 20–500 °C while cement paste underwent thermal shrinkage for temperatures higher than 150 °C.

The linear thermal expansion coefficients calculated using the $\varepsilon(T)$ functions from Fig. 2 are presented in Fig. 3 which makes possible to analyze the effect of temperature increase on length changes of both studied aluminosilicates in more details. The $\alpha(T)$ functions were increasing in the lower-temperature range, for NS up to approximately 400 °C, for EP to 300 °C. Then the linear thermal expansion coefficient of NS began to decrease so that at 800 °C it had similar value as at room-temperature, and finally in the temperature range of 800–1000 °C it was almost constant. On the other hand, the $\alpha(T)$ function of EP was only slightly decreasing in the temperature range of 300–700 °C, and then it decreased faster so that at 1000 °C it was similar as at room-temperature.

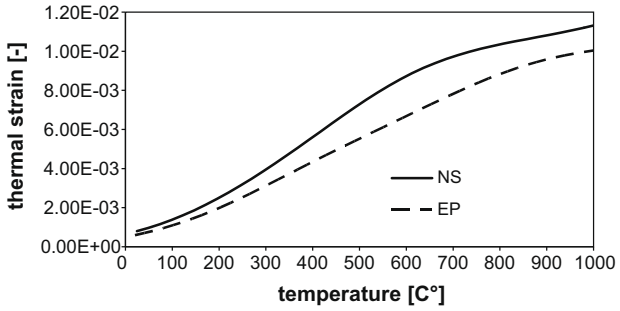

Fig. 2. Thermal strain of analyzed materials as function of temperature.

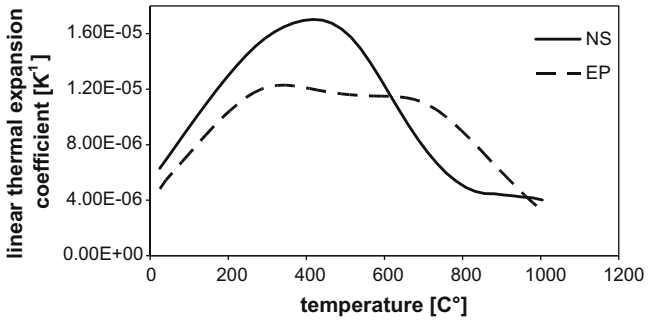

Fig. 3. Linear thermal expansion coefficient of analyzed materials as function of temperature.

The differences between the $\alpha(T)$ functions in Fig. 3 can be explained by the different behavior of the two materials used in the studied aluminosilicate composites as aggregates after their exposure to elevated temperatures. Electrical porcelain is characterized by low linear thermal expansion coefficient (6–$8 \times 10^{-6}\,K^{-1}$ in average) and no sudden volumetric changes in the temperature range up to 1000 °C [26,27]. Quartz, on the other hand, is subject of displacive phase transition from α (low) to β (high) modification at 573 °C [28]. The different quartz forms differ also in their structural response to increasing temperatures. While the thermal expansion coefficient of α-quartz is positive ($18 \times 10^{-6}\,K^{-1}$ in average, calculated using the data in [28,29]), it was found that β-quartz does not exhibit any significant thermal expansion from 573 °C up to 1000 °C [28,29] or possibly it even undergoes thermal shrinkage [30]. Thus, the electrical porcelain aggregates had clearly better prerequisites to compensate for the thermal shrinkage of aluminosilicate gel than quartz sand, in the temperature range of 573–1000 °C in particular.

The dependence of the linear thermal expansion coefficient on temperature of both studied materials was in a good qualitative agreement with the residual strength values measured in [12,13]. The fast decrease of $\alpha(T)$ of the material NS with quartz sand aggregates between 400 °C and 800 °C was well correlated with compressive strength which decreased more than four times in that temperature range. The 50% reduction in compressive strength of the material EP with electrical porcelain aggregates between 600 °C and 800 °C corresponded to the decrease of $\alpha(T)$ for temperatures above 700 °C. So, the thermal expansion properties of different aggregates played a significant role in the mechanical performance of the analyzed aluminosilicates. The important role of aggregates in that respect can also be supported by a comparison with the results obtained in [23]. While for the alkali activated slag concrete with basalt coarse aggregates from [23] the reduction in compressive strength between room-temperature and 800 °C was approximately 90%, for NS in [12] it was 80% and for EP in [13] only 70%. In the temperature range of 800–1200 °C the role of the type of aggregates was even more notable. The alkali activated slag concrete from [23] lost at 1200 °C its strength completely but quartz and electrical porcelain aggregates in [12,13] provided the necessary compounds for ceramic bond formation which caused the compressive strength to increase more than five times for both NS and EP.

The thermal expansion properties of alkali-activated aluminosilicate composites obtained in this paper can be compared with

common cementitious composites in a limited extent only as very few results were published until now. In [25], the total thermal strain of cement mortar at 500 °C was approximately 9×10^{-3}. This was 20% higher than for the aluminosilicate with quartz sand in this paper and almost 40% higher than for the material with electrical porcelain aggregates. The $\alpha(T)$ functions determined up to 1000 °C for cement mortar in [24] and for high performance concrete in [31] were similar in shape to the aluminosilicate material with quartz sand but 20–50% higher in the whole temperature range. As lower thermal strain generally results in lower thermal stress, thus in lower risk of failure of a building element subjected to one-sided heating, the thermomechanical behavior of the aluminosilicates studied in this paper can be characterized as mostly better than of Portland-cement based composites.

6. Conclusions

Experimental investigations presented in this paper showed that the thermal expansion properties of aggregates affected the thermomechanical behavior of the analyzed alkali-activated aluminosilicate composites in a significant way. The main findings can be summarized as follows:

- Contrary to the results obtained for geopolymers [20–22] and alkali activated slag pastes [23], no thermal shrinkage was observed up to 1000 °C; the thermal expansion mismatch between the contracting aluminosilicate gel and expanding aggregates resulted, for the aluminosilicate composites with both quartz sand and electrical porcelain aggregates, in positive values of the apparent linear thermal expansion coefficient α.
- Electrical porcelain aggregates were identified as a more desired solution from the point of view of thermomechanical properties of aluminosilicate composites; lower thermal strain and a smoother $\alpha(T)$ function were observed as compared with a similar composite produced using quartz sand. This was a consequence of better high-temperature volumetric stability of electrical porcelain, which is characterized by low linear thermal expansion coefficient and no sudden volumetric changes in the temperature range up to 1000 °C, while quartz is subject to a displacive phase transition from α to β modification at 573 °C. In addition, the different quartz forms differ also in their structural response to increasing temperatures.
- In a comparison with Portland-cement based composites the linear thermal expansion coefficient of both studied aluminosilicates was in the whole temperature range of 20–1000 °C significantly lower. As lower thermal strain generally results in lower thermal stress, and thus in lower risk of failure of a building element subjected to one-sided heating, their thermomechanical behavior can be characterized as better than Portland-cement based composites.
- The development of thermal strain with temperature was for both studied materials in a good correlation with the measurements of residual compressive strength presented before [12,13].

Acknowledgement

This research has been supported by the Ministry of Education, Youth and Sports of the Czech Republic, under Project No. MSM: 6840770031.

References

[1] Davidovits J. Geopolymers and geopolymeric materials. J Therm Anal 1989;35:429–41.
[2] Davidovits J. Geopolymers – inorganic polymeric new materials. J Therm Anal 1991;37:1633–56.
[3] Khale D, Chaudhary R. Mechanism of geopolymerization and factors influencing its development: a review. J Mater Sci 2007;42:729–46.
[4] Wang SD, Pu XC, Scrivener KL, Pratt PL. Alkali-activated slag cement and concrete: a review of properties and problems. Adv Cem Res 1995;7:93–102.
[5] Bakharev T, Sanjayan JG, Cheng YB. Effect of admixtures on properties of alkali-activated slag concrete. Cem Concr Res 2000;30:1367–74.
[6] Collins F, Sanjayan JG. Microcracking and strength development of alkali activated slag concrete. Cem Concr Compos 2001;23:345–52.
[7] Chang JJ, Yeih W, Hung CC. Effects of gypsum and phosphoric acid on the properties of sodium silicate-based alkali-activated slag pastes. Cem Concr Compos 2005;27:85–91.
[8] Palacios M, Puertas F. Effect of superplasticizer and shrinkage-reducing admixtures on alkali-activated slag pastes and mortars. Cem Concr Res 2005;35:1358–67.
[9] Palacios M, Puertas F. Effect of shrinkage-reducing admixtures on the properties of alkali-activated slag mortars and pastes. Cem Concr Res 2007;37:691–702.
[10] Jo BW, Park SK, Park MS. Strength and hardening characteristics of activated fly ash mortars. Mag Concr Res 2007;59:121–9.
[11] Shoaib MM, Ahmed SA, Balaha MM. Effect of fire and cooling mode on the properties of slag mortars. Cem Concr Res 2001;31:1533–8.
[12] Zuda L, Pavlík Z, Rovnaníková P, Bayer P, Černý R. Properties of alkali activated aluminosilicate material after thermal load. Int J Thermophys 2006;27:1250–63.
[13] Zuda L, Bayer P, Rovnaník P, Černý R. Mechanical and hydric properties of alkali-activated aluminosilicate composite with electrical porcelain aggregates. Cem Concr Compos 2008;30:266–73.
[14] Kong DLY, Sanjayan JG, Sagoe-Crentsil K. Factors affecting the performance of metakaolin geopolymers exposed to elevated temperature. J Mater Sci 2008;43:824–31.
[15] Shi C. Strength, pore structure and permeability of alkali-activated slag mortars. Cem Concr Res 1996;26:1789–99.
[16] Douglas E, Bilodeau A, Malhotra VM. Properties and durability of alkali-activated slag concrete. ACI Mater J 1992;89:509–16.
[17] Roy DM, Jiang W, Silsbee MR. Chloride diffusion in ordinary, blended and alkali-activated cement pastes and its relation to other properties. Cem Concr Res 2000;30:1879–84.
[18] Zuda L, Rovnaník P, Bayer P, Černý R. Thermal properties of alkali activated slag subjected to high temperatures. J Build Phys 2007;30:337–50.
[19] Melo Neto AA, Cincotto MA, Repette W. Drying and autogenous shrinkage of pastes and mortars with activated slag cement. Cem Concr Res 2008;38:565–74.
[20] Duxson P, Lukey GC, van Deventer JSJ. Thermal evolution of metakaolin geopolymers: part 1 – physical evolution. J Non-Cryst Solids 2006;352:5541–55.
[21] Duxson P, Lukey GC, van Deventer JSJ. Physical evolution of Na-geopolymer derived from metakaolin up to 1000 °C. J Mater Sci 2007;42:3044–54.
[22] Subaer, van Riessen A. Thermo-mechanical and microstructural characterisation of sodium-poly(sialate-siloxo) geopolymers. J Mater Sci 2007;42:3117–23.
[23] Guerrieri M, Sanjayan JG, Collins FG. Residual compressive behavior of alkali activated concrete exposed to elevated temperatures. Fire Mater 2009;33:51–62.
[24] Toman J, Koudelová P, Černý R. A measuring method for the determination of linear thermal expansion of porous materials at high temperatures. High Temp-High Press 1999;31:595–600.
[25] Fu YF, Wong YL, Poon CS, Tang CA, Lin P. Experimental study of micro/macro crack development and stress–strain relations of cement-based composite materials at elevated temperatures. Cem Concr Res 2004;34:789–97.
[26] Amigo JM, Clausell JV, Esteve V, Delgado JM, Reventos MM, Ochando LE, et al. X-ray powder diffraction phase analysis and thermomechanical properties of silica and alumina porcelains. J Eur Ceram Soc 2004;24:75–81.
[27] Kamseu E, Leonelli C, Boccaccini D. Non-contact dilatometry of hard and soft porcelain compositions. J Therm Anal Calorim 2007;88:571–6.
[28] Carpenter MA, Salje EKH, Graeme-Barber A, Wruck B, Dove MT, Knight KS. Calibration of excess thermodynamic properties and elastic constant variations associated with the $\alpha \rightarrow \beta$ phase transition in quartz. Am Mineral 1998;8:2–22.
[29] Lakshtanov DL, Sinogeikin SV, Bass JD. High-temperature phase transitions and elasticity of silica polymorphs. Phys Chem Miner 2007;34:11–22.
[30] Huang LP, Kieffer J. Structural origin of negative thermal expansion in high-temperature silica polymorphs. Phys Rev Lett 2005;95:215901.
[31] Toman J, Černý R. Thermal and hygric expansion of high performance concrete. Acta Polytech 2001;41:2–4.